CHEMICAL ENGINEERING TRANSACTIONS

VOL. 61, 2017

A publication of AIDIC
The Italian Association
of Chemical Engineering
Online at www.aidic.it/cet

Guest Editors: Petar S Varbanov, Rongxin Su, Hon Loong Lam, Xia Liu, Jiří J Klemeš

ISBN 978-88-95608-51-8; **ISSN** 2283-9216

DOI: 10.3303/CET1761253

Highly Sensitive Ratiometric Fluorescent Probe for the Detection of Mercury Ions

Yanfei Yue[a], Zhao Gao[a,b], Lian Chen[c], Rongxin Su[a,*], Wei Qi[a], Zhimin He[a]

[a]State Key Laboratory of Chemical Engineering, Tianjin Key Laboratory of Membrane Science and Desalination Technology, School of Chemical Engineering and Technology, Tianjin University, Tianjin 300072, PR China
[b]College of Life Science, Dalian Minzu University, Dalian 116600, PR China.
[c]Research Center of Hunan Entry-Exit Inspection and Quarantine Bureau, Changsha 410001, PR China
surx@tju.edu.cn

An effective dual-emission fluorescent probe combining gold nanoclusters (AuNCs) and carbon dots (CDs) was fabricated for the detection of mercury ions (Hg^{2+}). CDs doped into silica nanoparticles exhibited a reference fluorescence signal, while the outer AuNCs layer stabilized by bovine serum albumin (BSA) was extremely sensitive to Hg^{2+}. This probe selectively detected Hg^{2+} in a good linear range from 0.43 to 39 μM and a detection limit (signal-to-noise ratio is 3) of 81 nM. The increase in the Hg^{2+} concentration was accompanied by the colour change from reddish violet to blue. This method exhibited several advantages of facile preparation and operation and high selectivity and sensitivity. This dual-emission fluorescent probe has significant potential for the ‘‘naked eye’’ detection of Hg^{2+}.

1. Introduction

Pollution by heavy metals leads to severe environmental and ecological problems (Chen and Bi, 2016). Mercury ion (Hg^{2+}) is one of the most toxic heavy metals, which is widespread in air, water, and soil. The accumulation of mercury in the human body can cause severe damage to the central nervous system, resulting in various cognitive and motor disorders, as well as the Minamata disease. Besides, the presence of Hg^{2+} in the human body also leads to severe toxic effects on the human hematopoietic system, respiratory system, and the kidneys. Hence, it is imperative to develop a facile and sensitive probe for the detection of Hg^{2+}. Recently, the optical methods, especially fluorescence-based analytical methods, have been employed for the analysis of Hg^{2+} in real water samples with good results (Kim et al., 2012).

Ratiometric fluorescence method demonstrates several advantages for the measurement of the fluorescence intensities at two wavelengths. Compared to the typical fluorescence quenching probe based on a single fluorescence signal, the ratiometric fluorescent probe can decrease or eliminate the operational errors caused by the substrate, by the external environment, by the changes in the instrument conditions or other factors, as well as improve the measurement accuracy of the results (Chen et al., 2013).

Dye-doped silica nanoparticles have been developed as ratiometric fluorescent probes, which have been widely used for selective determination because of their good chemical and colloidal stabilities, well-developed surface coupling technology, and low toxicity (Zhang et al., 2011). Zong et al. (2011) reported a nanoprobe, with a dye-doped silica core serving as a reference signal, thus providing a built-in correction for environmental effects, and a response dye was covalently grafted on the silica nanoparticle surface using a chelating reagent for Cu^{2+}.

Fluorescence carbon dots (CDs) represent a new class of carbon nanomaterials, which overcome some of the limitations of traditional quantum dots. Carbon dots are non-toxic and easy to implement for surface functionalization, in addition to their excellent optical performance and good biocompatibility (Gao et al., 2015). As another important fluorescent material, gold nanoclusters (AuNCs) demonstrate several advantages, e.g., non-toxicity, near-infrared emission, good biological compatibility, and narrow emission spectra (Xie et al., 2010). Because of these advantages of above materials, AuNCs and CDs were combined to afford a

Please cite this article as: Yue Y., Gao Z., Chen L., Su R., Qi W., He Z., 2017, Highly sensitive ratiometric fluorescent probe for the detection of mercury ions, Chemical Engineering Transactions, 61, 1531-1536 DOI:10.3303/CET1761253

composite probe based on silica nanoparticles, which was applied as a ratiometric fluorescent probe for Hg^{2+} detection.

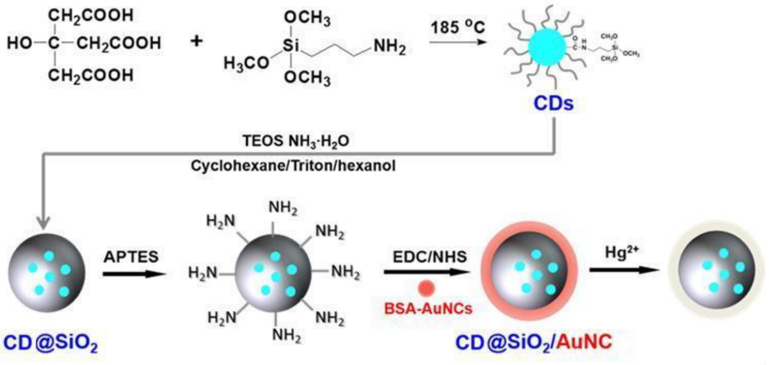

Figure 1: Schematic for the synthesis and application of the dual-emission fluorescent probe CD@SiO₂/AuNC. In the presence of Hg^{2+}, the fluorescence intensity corresponding to the outside layer (AuNCs) of the hybrid probe decreased, whereas that of the inside layer (CDs) remained constant

Figure 1 shows the preparation of the hybrid ratiometric probe herein and the working principle for the visual detection of Hg^{2+}. Herein, CDs were prepared by the thermal pyrolysis of anhydrous citric acid and 3-aminopropyl trimethoxysilane (APTMS). Subsequently, the CD-doped fluorescent silica core (CD@SiO_2) was synthesized by a reverse microemulsion method. Gold nanoclusters were stabilized by bovine serum albumin (BSA–AuNCs), which were then covalently connected with amino-modified CD@SiO_2 nanoparticles after the surface was activated by a carboxyl-group-based activating reagent, e.g., 1-ethyl-3-[3-(dimethylamino)propyl]-carbodiimide (EDC). In this dual-emission hybrid fluorescent probe, the inside CDs provided the reference fluorescence signal, while the outer BSA–AuNCs layer was extremely reactive to Hg^{2+}.

2. Materials and methods

Citric acid, hydrochloroauric acid, APTMS, 3-aminopropyltriethoxysilane (APTES), N-hydroxysuccinimide (NHS), and EDC were obtained from Aladdin Reagent Company (Shanghai, China). BSA was purchased from Sigma-Aldrich (Beijing, China). Mercuric chloride was purchased from J&K Scientific Company (Beijing, China). All other chemicals were of analytical grade and were commercially obtained. Ultrafiltration centrifuge tubes with a molecular weight cut-off of 3,500 Da were obtained from Sigma-Aldrich (Beijing, China).

2.1 Synthesis of fluorescent CDs

CDs were synthesized by the one-step pyrolysis of citric acid at high temperature. In a typical synthesis procedure, 10 mL of APTMS was added in a 100 mL three-neck round-bottom flask. Then, the flask was heated to 185°C using an electric heating jacket and 0.5 g of anhydrous citric acid was added into the flask. After 1 min, the colour of the reaction system changed to dark green. Subsequently, the flask was cooled to room temperature. The reaction solution was extracted five times using petroleum ether with the same volume. Finally, freshly prepared CDs were obtained as the dark green bottom liquid after extraction.

2.2 Preparation of CD@SiO_2

The reverse microemulsion method was employed to synthesize fluorescent CD-doped silica nanoparticles. First, a W/O microemulsion solution was prepared by mixing 1.77 mL of TX-100, 7.7 mL of cyclohexane, 1.8 mL of n-hexanol, and 380 μL of water. Second, the system was vigorously stirred for 10 min to attain stability and homogeneity. Third, 50 μL of TEOS was added. After mixing, 25 μL of freshly prepared CDs was added. Next, with gentle stirring, 200 μL of the 25 wt% ammonia solution was added, and the reaction was allowed to stir for 24 h at room temperature. Three times the volume of isopropyl alcohol was added, followed by centrifugation and washing with ethanol and water several times until no fluorescence signal was observed for the supernatant. Finally, the CD@SiO_2 nanoparticles were dispersed in ethanol by ultrasonication. At the same time, silica nanoparticles were prepared without CDs as the control sample.

2.3 Synthesis of AuNCs

All of the glassware was washed with aqua regia (HCl/HNO_3 volume ratio = 3:1) before use. In a typical experiment, an aqueous $HAuCl_4$ solution (1 mL, 10 mM) was first added to the BSA solution (1 mL, 50 mg/mL) under vigorous stirring for 2–3 min. Then, a 1 M NaOH solution was added to attain a pH of 11, and the reaction was allowed to stir vigorously at 40 °C for 12 h. The as-synthesized AuNCs were dialyzed in a membrane tubing with an MWCO of 3500 Da against 1 L of continuously stirred ultrapure water at 4 °C. After 36 h, the tubing contents (AuNCs) were collected, and the solution was stored at 4 °C for subsequent use.

2.4 Synthesis of dual-emission fluorescent probe (CD@SiO_2/AuNC)

The first step involves the amination of CD@SiO_2. First, the as-prepared CD@SiO_2 nanoparticles were dispersed in 20 mL of ethanol with a final concentration of 0.1 mg/mL. Second, 100 µL of APTES was rapidly added. Next, the resulting solution was heated to the reflux temperature and stirred for 24 h. Finally, the nanoparticles thus obtained were separated by centrifugation and dispersed in a phosphate buffer (10 mM, pH 7.0). The second step involves the grafting of AuNCs on CD-doped silica nanoparticles. 0.1 mL of the as-prepared BSA–AuNCs solution was diluted to 1 mL using a phosphate buffer (10 mM, pH 7.0). Then, 0.5 mL of EDC (100 mM) and 0.5 mL of an NHS (400 mM) solution were added and stirred for 0.5 h at room temperature. After that, 1 mL of the as-prepared CD@SiO_2 was added in the mixed solution and stirred for 12 h under 4°C.

2.5 Fluorescence detection of mercury ions

To detect Hg^{2+}, different solutions with increasing Hg^{2+} concentration were added into 3 mL of the CD@SiO_2/AuNC solution. Then, fluorescence spectra were recorded at an excitation wavelength of 380 nm with an excitation or emission slit width of 10 nm. The selectivity for Hg^{2+} detection was investigated by the addition of other interferences, following the same procedure. All experiments were performed at room temperature and repeated at least three times.

3. Results and discussion

3.1 Structural and optical characterization of CD@SiO_2

As shown in the UV–vis spectrum of CD@SiO_2 in Figure 2a, a weak absorption peak was observed at 342 nm, indicating that CDs are successfully coated inside of the SiO_2 nanoparticles. Next, the fluorescence properties of the as-prepared CD@SiO_2 were further examined (Figure 2b). The maximum emission peaks corresponding to fluorescent CD@SiO_2 blue-shifted to 455 nm as compared with that observed for CDs (Zhao et al., 2004). Figure 2c and 2d show the typical SEM and TEM images of as-prepared CD@SiO_2, respectively. The size distribution of CD@SiO_2 was 40–70 nm. After doping with SiO_2 nanoparticles, CD@SiO_2 could be dispersed in water and ethanol and still exhibited blue fluorescence under UV light (Figure 2c, inset). Both FTIR spectra and time-correlated single photon counting (TCSPC) were used to characterized for CD@SiO_2 and SiO_2. As compared to only CDs, the CD@SiO_2 complex exhibited a shorter lifetime.

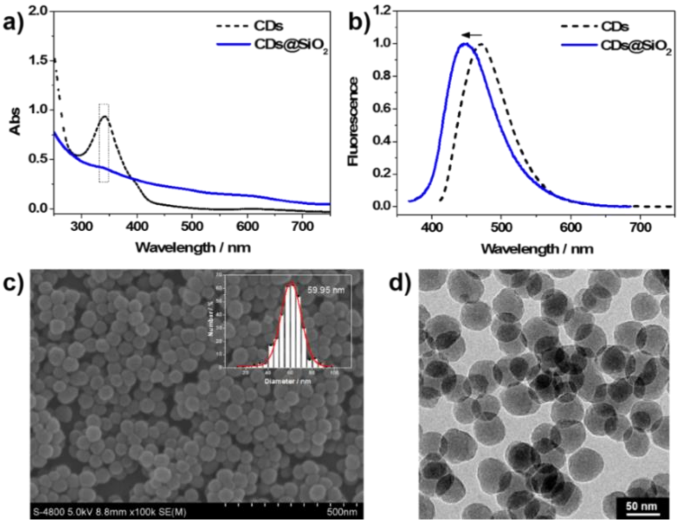

Figure 2: UV–vis (a) and fluorescence emission spectra (b) of CDs and CD@SiO_2. SEM (c) and TEM images (d) of CD@SiO_2. Inset in (c) shows the size distributions of CD@SiO_2 according to the SEM image

3.2 Structural and optical characterization of CD@SiO$_2$/AuNC

Figure 3 shows the TEM and HRTEM images of the hybrid probe, i.e., CD@SiO$_2$/AuNC. After the formation of the outer BSA–AuNCs layer, the CD@SiO$_2$/AuNC surface was rougher than the CD@SiO$_2$ surface, with a size of approximately 1 nm. The optical characteristics of CD@SiO$_2$/AuNC were further examined by UV–vis and fluorescence spectroscopy. As shown in Figure 3c, BSA–AuNCs exhibited a characteristic absorption peak at 280 nm, corresponding to protein adsorption, whereas CD@SiO$_2$ exhibited a peak at 342 nm, corresponding to CDs. CD@SiO$_2$/AuNC exhibited peaks at 280 nm and 342 nm, indicating that BSA–AuNCs are decorated on the CD@SiO$_2$ surface. With irradiation using a UV lamp at a wavelength of 365 nm, the aqueous solution of CD@SiO$_2$/AuNC exhibited red luminescence (inset photograph of Figure 3d). The CD@SiO$_2$/AuNC nanohybrids emitted two fluorescence peaks at 455 nm and 650 nm, with different colors, under a single wavelength of 380 nm. The red fluorescence corresponded to BSA–AuNCs (Tao et al., 2013), with sensitive quenching in the response to Hg^{2+}, while the blue fluorescence corresponded to the CDs, acting as the internal reference.

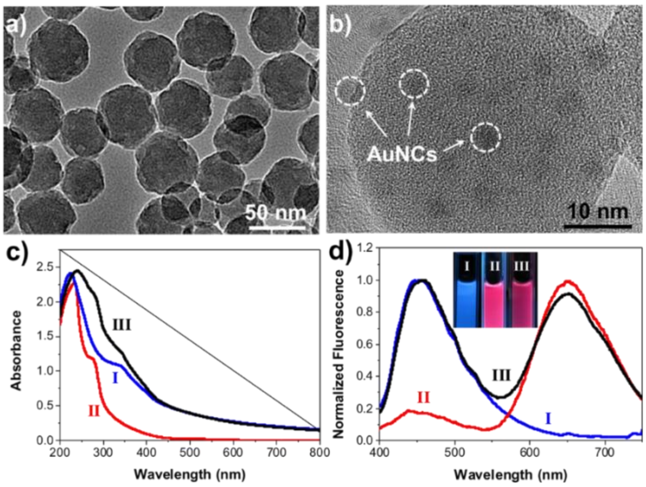

Figure 3: TEM (a) and HRTEM (b) images of the CD@SiO$_2$/AuNC nanohybrid. (c) UV–vis spectra of the CD@SiO$_2$, BSA–AuNCs, and ratiometric hybrid probe particles. (d) Normalized fluorescence emission spectra of the CD@SiO$_2$ (I), BSA–AuNCs (II), and ratiometric hybrid particles (III). Inset: photographs of the three samples under a 365 nm UV lamp

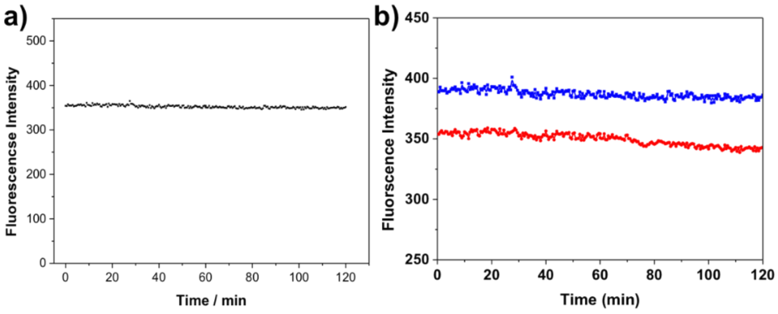

Figure 4: Stabilities of the fluorescence intensities of CD@SiO$_2$ at 455 nm excited by 350 nm (a), CD@SiO$_2$/AuNCs at 455 nm and 650 nm excited by 380 nm (b)

The stability of CD@SiO$_2$ was tested by measuring the fluorescence emission intensity at 455 nm under an excitation light irradiation of 350 nm. As shown in Figure 4a, with prolonged illumination, the fluorescence intensity of CD@SiO$_2$ remained unchanged within 2h, indicating high stability and anti-fluorescence photobleaching ability. The fluorescence intensity of the CD@SiO$_2$/AuNC hybrid probe remained unchanged under continuous illumination by 455 nm and 650 nm for up to 2 h (Figure 4b). The change in the fluorescence intensity was less than 5 % within testing for 2 h, indicative the good stability of the ratiometric fluorescent probes for promising applications in quantitative determination.

3.3 Fluorescence detection of mercury ions

The developed dual-emission hybrid ratiometric probe was used to detect Hg^{2+} utilizing fluorescence emission intensities. Figure 5 shows the recorded response. The results confirm the effective fluorescence quenching of AuNCs by Hg^{2+}, related to high-affinity metallophilic interactions. The probe exhibited two emission peaks at 455 nm and 650 nm under a single wavelength excitation of 380 nm, which are emitted from the CDs on the surface and AuNCs embedded within the silica nanoparticles. With the addition of Hg^{2+}, the intensity of the red emission at 650 nm (Fr) was gradually decreased, while that of the blue emission at 455 nm (Fb) remained constant, acting as an internal reference. This process was accompanied by an obvious colour change from reddish violet to blue (Figure 5a, inset). The ratios of fluorescence intensities at 455 and 650 nm (Fr/Fb) exhibited good linearity with increasing Hg^{2+} concentrations in the range from 0.43 to 39 μM (Figure 5b). The linear regression equation was Fr/Fb = –0.01894C + 0.9333, and the detection limit was 81 nM (signal-to-noise ratio is 3). To examine probe reproducibility, 10 parallel measurements using a solution with a certain Hg^{2+} concentration were conducted, and a relative standard deviation of 2.67 % was obtained, suggesting that this probe is suitable for quantitative determination.

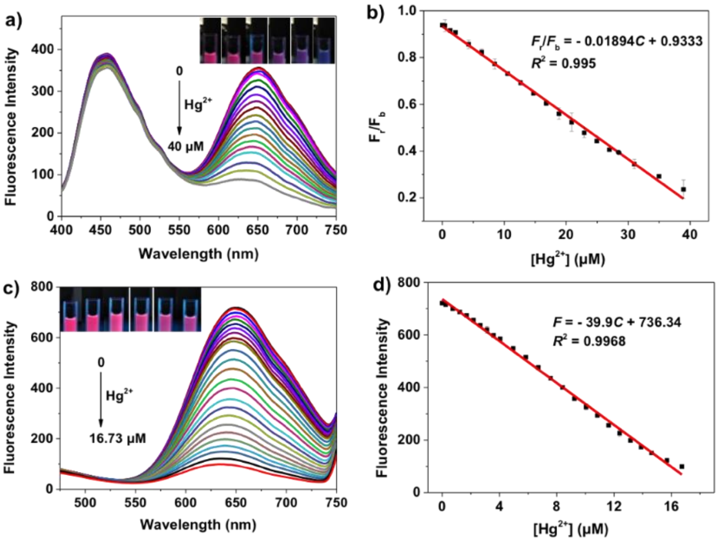

Figure 5: Fluorescence spectra (a, c) and the corresponding working curve (b, d) of the ratiometric probe (a, b) and pure BSA–AuNCs (c, d) upon the addition of different Hg^{2+} concentrations. Inset: optical images for the fluorescence color of the ratiometric probe in the presence of Hg^{2+}. Fluorescence photographs were recorded under a UV lamp (365 nm)

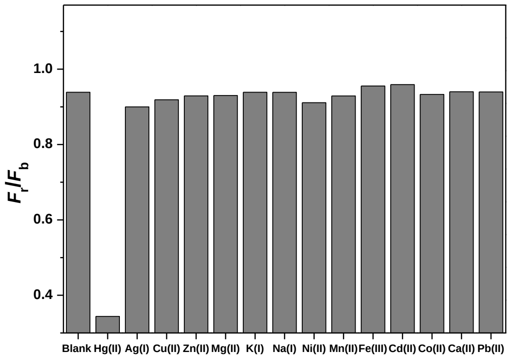

Figure 6: Ratiometric fluorescence responses of the CD@SiO_2/AuNC sensor to various substances (1 mM concentration)

As a contrast experiment, BSA-AuNCs were separately used as the fluorescent probe for Hg^{2+} detection (Figure 5). For a Hg^{2+} concentration range of 0.24–16.8 μM, the fluorescence intensity of AuNCs and Hg^{2+} concentration exhibited good linearity (R^2 = 0.998), with a detection limit of 52 nM. The detection range of dual-emission hybrid ratiometric probe was broader than the individual BSA-AuNCs detection. Besides, Chen et al. (2014) have used a chitosan-functionalized AuNP for colorimetric detection and obtained a detection range of 9–50 μM. Lee et al. (2013) have utilized the fluorescence of rhodamine hydrazone derivatives and obtained a detection range of 0.28–0.8 μM. The sensitivity of the developed method is comparable or superior to those of the above-mentioned methods for the determination of Hg^{2+} in solutions. Hence, the dual-emission fluorescent probe exhibited a higher detection limit and a wider linear range, and it can be suitable for naked eye visual inspection.

In addition to the sensitivity requirement, high specificity is also important in a majority of detection scenarios, especially for actual sample detection. To evaluate the specificity of this ratiometric probe, interference experiments in the presence of common metallic ions, e.g., K^+, Na^+, Ca^{2+}, Mg^{2+}, Zn^{2+}, Cu^{2+} and Fe^{3+}, were carried out under the same conditions. Marked fluorescence changes were observed after the addition of 30 μM metallic ion solutions. As shown in Figure 6, only Hg^{2+} clearly affected the fluorescence intensity range of the $CD@SiO_2/AuNC$ sensor, indicating that the probe demonstrates excellent selectivity for Hg^{2+}.

4. Conclusions

In summary, siloxane-functionalized carbon quantum dots were successfully synthesized using long-chain amino siloxane. Then, the functionalized carbon quantum dots formed carbon dot–silica composite particles, with an average particle size of approximately 60 nm. A facile dual-emission fluorescent probe was constructed by the hybridization of gold nanoclusters and carbon-dot-based silica particles and utilized for the visual detection of Hg^{2+}. The $CD@SiO_2/AuNC$ hybrid probe can be used for the quantification of Hg^{2+} in solutions on the basis of the ratiometric fluorescence measurement. The probe exhibited facile operation, high selectivity, and sensitivity and provided potential for the detection of Hg^{2+} by the naked eye.

Acknowledgments

This study was supported by the Ministry of Science and Technology of China (No. 2012YQ090194), the Natural Science Foundation of China (No. 51473115), and the Natural Science Foundation of Tianjin (No. 16JCZDJC37900).

References

Chen J., Bi W., 2016, Monitoring Technology of Trace Heavy Metals in Seawater Based on Spectrophotometry, Chemical Engineering Transactions, 55, 313-318.

Chen T., Hu Y., Cen Y., Chu X., Lu Y., 2013, A Dual-Emission Fluorescent Nanocomplex of Gold-Cluster-Decorated Silica Particles for Live Cell Imaging of Highly Reactive Oxygen Species, Journal of the American Chemical Society, 135(31), 11595-11602.

Chen Z., Zhang C., Tan Y., Zhou T., Ma H., Wan C., Lin Y., Li K., 2014, Chitosan-Functionalized Gold Nanoparticles for Colorimetric Detection of Mercury Ions Based on Chelation-Induced Aggregation, Microchimica Acta, 182(3-4), 611-616.

Gao Z., Wang L., Su R., Huang R., Qi W., He Z., 2015, A Carbon Dot-Based "Off-On" Fluorescent Probe for Highly Selective and Sensitive Detection of Phytic Acid, Biosensors & Bioelectronics, 70, 232-238.

Kim H.N., Ren W.X., Kim J.S., Yoon J., 2012, Fluorescent and Colorimetric Sensors for Detection of Lead, Cadmium, and Mercury Ions, Chemical Society Reviews, 41(8), 3210-3244.

Lee H.Y., Swamy K.M.K., Jung J.Y., Kim G., Yoon J., 2013, Rhodamine Hydrazone Derivatives Based Selective Fluorescent and Colorimetric Chemodosimeters for Hg^{2+} and Selective Colorimetric Chemosensor for Cu^{2+}, Sensors and Actuators B: Chemical, 182, 530-537.

Tao Y., Lin Y., Ren J., Qu X., 2013, A Dual Fluorometric and Colorimetric Sensor for Dopamine Based on BSA-Stabilized Au Nanoclusters, Biosensors & Bioelectronics, 42, 41-46.

Zhao X., Bagwe R.P., Tan W., 2004, Development of Organic-Dye-Doped Silica Nanoparticles in a Reverse Microemulsion, Advanced Materials, 16, 173-176.

Xie J., Zheng Y., Ying J.Y., 2010, Highly Selective and Ultrasensitive Detection of Hg^{2+} Based on Fluorescence Quenching of Au Nanoclusters by Hg^{2+}-Au^+ Interactions, Chemical Communications, 46(6), 961-963.

Zhang K., Zhou H., Mei Q., Wang S., Guan G., Liu R., Zhang J., Zhang Z., 2011, Instant Visual Detection of Trinitrotoluene Particulates on Various Surfaces by Ratiometric Fluorescence of Dual-Emission Quantum Dots Hybrid. Journal of the American Chemical Society, 133(22), 8424-8427.

Zong C., Ai K., Zhang G., Li H., Lu L., 2011, Dual-Emission Fluorescent Silica Nanoparticle-Based Probe for Ultrasensitive Detection of Cu^{2+}. Analytical Chemistry, 83(8), 3126-3132.